Effects of Structural Modes on Vibratory Force Determination by the Pseudoinverse Technique

James A. Fabunmi*
University of Maryland, College Park, Maryland

The accuracy and effectiveness of the pseudoinverse technique as a means of determining the operating vibratory loads on a structural system, from acceleration mobilities obtained by modal superposition, can be severely undermined by lack of proper consideration of the participation of the structural modes at the frequency of interest. Methods of linear algebra and modal analysis are used to establish the limitations of this technique with regard to the number of independent forces determinable at a given frequency in relation to the number and significance of structural modes participating in the response at that frequency. Results of numerical calculations based on two uniform beams, one cantilevered and the other free-free, show that for an assumed level of random error in the acceleration mobility matrix, the accuracy of the determined forces correlates well with a parameter that is related to the number of modes contributing to the response of the structure at a given frequency.

Nomenclature

A_{ijn}	= ijth modal acceleration of the nth mode
EI	= flexural rigidity of uniform beam
E_{ij}	= random error in ijth mobility
$\{F(\omega)\},\{F'\}$	= vectors of excitation and determined forces, respectively
$G_n(\omega)$	= complex modal function
g_n	= damping coefficient of nth mode
i	= complex number
i,j,r,n,p,q,s	= indices
L	= beam length
M	= number of response coordinates, mass per unit length of beam
N_E,N_R	= number of elastic and rigid-body modes, respectively
$(RAC)_{ij}$	= ijth rigid-body acceleration coefficient
S	= number of sample calculations
x	= position variable
x_j	= jth position coordinate
$Y_{ij}(\omega)$	= ijth element of mobility matrix
$\lvert Y\rvert_j$	= magnitude of largest element in the jth column of the mobility matrix $[Y(\omega)]$
$\{Y_j(\omega)\}$	= vector of jth column of mobility matrix $[Y(\omega)]$
$\{y(\omega)\}$	= vector of response accelerations
$[Y(\omega)]$	= matrix of acceleration mobilities
$\alpha_{A,p}$	= norm of pth row of $[\alpha_A]$
$\alpha_{A,pi}$	= pith element of $[\alpha_A]$
$[\alpha_F],[\alpha_A]$	= matrices defined in text; see Eq. (11)
$\alpha_{F,p}$	= norm of pth row of $[\alpha_F]$
$\alpha_{F,pj}$	= pjth element of $[\alpha_F]$
α_{nj},β_j,K_n	= coefficients, defined in text; see Eqs. (7,8)
$\{\beta\}$	= vector comprised of elements β_j
β_n	= coefficient defined in Eq. (17)
γ	= error level in mobilities, %
$\epsilon(\omega)$	= parameter equals lesser of $\epsilon_F(\omega)$ and $\epsilon_A(\omega)$; see Eq. (14)
$\epsilon_F(\omega),\epsilon_A(\omega)$	= log of norm ratios, defined in Eq. (13)
$\zeta(\omega)$	= average error of force determination
ρ_j	= random number $(-1\le\rho_j\le 1)$
ϕ_n,ϕ_n^C,ϕ_n^F	= element of nth mode shape function (superscripts C,F indicate cantilever and free-free beams, respectively)
ψ^E,ψ^R	= elements of elastic and rigid-body orthonormal modes, respectively
$\omega,\bar{\omega}$	= frequency, dimensionless frequency
Ω_n	= natural frequency of nth mode

Received Feb. 8, 1985; presented as Paper 85-0784 at the AIAA 26th Structures, Structural Dynamics and Materials Conference, Orlando, FL, April 15-17, 1985; revision received July 18, 1985.

*Assistant Professor, Aerospace Engineering.

Introduction

THE vector of response accelerations $\{y(\omega)\}$ of a linear structure that is subjected to steady forced vibrations is related to the vector of excitation forces $\{F(\omega)\}$ through the matrix of acceleration mobilities $[Y(\omega)]$, as stated in Eq. (1):

$$\{y(\omega)\}=[Y(\omega)]\{F(\omega)\} \tag{1}$$

It is a simple matter to measure the acceleration response of any part of a structure under operating conditions. Computers and fast Fourier transform (FFT) analyzers have made the direct measurements of the elements of the acceleration mobility matrix a routine activity in vibration testing of structures.[1-3] It would appear straightforward simply to invert Eq. (1) in order to predict the excitation forces acting on a known structure. The results of the process can be enhanced by making acceleration measurements at many more locations than there are forces to be determined, thus requiring a generalized pseudoinversion of the rectangular mobility matrix,

$$\{F(\omega)\}=([Y(\omega)]^{*T}[Y(\omega)])^{-1}[Y(\omega)]^{*T}\{y(\omega)\} \tag{2}$$

where $[\ ]^{*T}$ is the complex conjugate transpose of the indicated matrix and $(\ )^{-1}$ is the inverse of a square matrix.

Indeed, much research has been done on the application of the pseudoinverse technique for the determination of external vibratory loads on known structures. Ellis[4] studied the methods of determining wind loads on flexible buildings, Flannelly and Bartlett[5,6] demonstrated the technology of force determination on a model helicopter and, subsequently, Flannelly et al.[7] implemented the technique on a full-scale helicopter (see also Ref. 8). In an attempt to establish the feasibility of the technique for determining forces on turbine blades, Ewins and Hillary[9] studied a cantilevered beam. Some of these applications and approaches yielded more accurate results than others. Insufficient accuracy of the measured mobility and accelertation data, ill conditioning of the mobility matrix, and insufficient number of acceleration measurement locations were some of the reasons given for poor accuracy of the force determination in a number of applications.

In this paper, some fundamental concepts of linear algebra and modal analysis are used to examine the implications of the pseudoinversion of the mobility matrix in the presence of random errors typical of measured data. First, some theoretical observations are made; then numerical calculations of the forced response of two uniform beams—one cantilevered and the other freely suspended—are used to illustrate the practical aspects of the theoretical results.

Theory

Let the ijth element of the acceleration mobility matrix be represented by a truncated series of contributions from the rigid-body and elastic modes of the structure[5,6];

$$Y_{ij}(\omega) = (RAC)_{ij} + \sum_{n=1}^{N_E} A_{ijn} G_n(\omega) \tag{3}$$

$G_n(\omega)$ is a complex valued function of frequency ω and properties of the nth elastic mode. For hysteretically damped structures,

$$G_n(\omega) = -(\omega^2/\Omega_n^2)/[(1-\omega^2/\Omega_n^2) + ig_n] \tag{4}$$

where Ω_n and g_n are the natural frequency and damping coefficient of the nth elastic mode, respectively [i in Eq. (4) is $\sqrt{(-1)}$]. A_{ijn} is the ijth modal acceleration of the nth elastic mode and can be written as

$$A_{ijn} = \psi_{ni}^E \psi_{nj}^E \tag{5}$$

where ψ_{ni}^E and ψ_{nj}^E are the ith and jth elements of the nth elastic orthonormal modes, respectively. $(RAC)_{ij}$, which can be regarded as the rigid-body acceleration coefficient relating rigid-body accelerations at coordinate i to excitation at coordinate j, can also be written as a sum of contributions from products of rigid-body orthonormal mode elements, provided that all coordinates and directions are defined with respect to a principal axis system, with origin at the c.m. of the structure.[10] So,

$$(RAC)_{ij} = \sum_{r=1}^{N_R} \psi_{ri}^R \psi_{rj}^R \tag{6}$$

ψ_{ri}^R and ψ_{rj}^R are the ith and jth elements of the rth rigid-body orthonormal modes, respectively. N_R is the number of rigid-body orthonormal modes participating in the response. If the structure is restrained from any rigid-body motions, $N_R=0$. The value of N_R for a freely suspended structure is influenced by the location and direction of the response and excitation pair ij (see Ref. 10 for a detailed treatment of rigid-body orthonormal modes). The number of elastic modes retained in Eq. (3), N_E, is dependent on the frequency range of interest. Generally, N_E is selected such that the contributions of elastic modes starting from N_E+1 are negligible.

If the elements of the jth column of the acceleration mobility matrix are arranged to form an $(M\times 1)$ vector $\{Y_j(\omega)\}$, where M is the number of response locations, then Eqs. (3-5) can be used to express this vector as

$$\underset{(M\times 1)}{\{Y_j(\omega)\}} \equiv \begin{Bmatrix} Y_{1j}(\omega) \\ Y_{2j}(\omega) \\ \vdots \\ Y_{Mj}(\omega) \end{Bmatrix} = \sum_{n=1}^{N_R+N_E} \alpha_{nj}\{\psi\}_n \tag{7}$$

where

$$\alpha_{nj} = \begin{cases} \psi_{nj}^R, & n=1,2,\ldots,N_R \\ \psi_{nj}^E G_n(\omega), & n=N_R+1,\ N_R+2,\ldots,N_R+N_E \end{cases}$$

and

$$\{\psi\}_n = \begin{cases} \{\psi^R\}_n, & n=1,2,\ldots,N_R \\ \{\psi^E\}_n, & n=N_R+1,\ N_R+2,\ldots,N_R+N_E \end{cases}$$

$\{\psi^R\}_n$ and $\{\psi^E\}_n$ are the $(M\times 1)$ vectors of the nth rigid-body and elastic orthonormal modes, respectively.

From considerations of linear algebra, the inverse $([Y(\omega)]^{*T}[Y(\omega)])^{-1}$ in Eq. (2) is feasible if all the columns and at least N_F rows of the $(M\times N_F)$ rectangular matrix $[Y(\omega)]$ are linearly independent. In order that the columns of $[Y(\omega)]$ be linearly independent, the sum

$$\sum_{j=1}^{N_F} \beta_j\{Y_j(\omega)\}$$

must not vanish unless all the coefficients β_j vanish identically. If any number N_b nonzero coefficients β_j exist such that

$$\sum_{j=1}^{N_F} \beta_j\{Y_j(\omega)\} = \{0\}$$

then at least N_b columns of the $[Y(\omega)]$ matrix are linearly dependent. From Eq. (7),

$$\sum_{j=1}^{N_F} \beta_j\{Y_j(\omega)\} = \sum_{n=1}^{N_R+N_E} K_n\{\psi\}_n \tag{8}$$

where

$$K_n = \sum_{j=1}^{N_F} \alpha_{nj}\beta_j$$

Since the vectors $\{\psi\}_n$ are orthonormal modes of the structure, they are linearly independent, so that the right-hand side of Eq. (8) can only vanish when all the K_n vanish for $n=1,2,\ldots,N_R+N_E$; that is, when

$$\sum_{j=1}^{N_F} \alpha_{nj}\beta_j = 0 \ \text{ for } \ n=1,2,\ldots,N_R+N_E \tag{9}$$

The condition in Eq. (9) is a homogeneous matrix equation of the form

$$[\alpha_F]\{\beta\} = \{0\} \tag{10}$$

$\{\beta\}$ is an $(N_F\times 1)$ vector of numbers β_j, while $[\alpha_F]$ is an $[(N_R+N_E)\times N_F]$ matrix, which can be written out as

$$[\alpha_F] = \begin{bmatrix} \psi_{11}^R & \psi_{12}^R & \cdot\ \cdot & \psi_{1N_F}^R \\ \cdot & \cdot & \cdot\ \cdot & \cdot \\ \cdot & \cdot & \cdot\ \cdot & \cdot \\ \psi_{N_R1}^R & \psi_{N_R2}^R & \cdot\ \cdot & \psi_{N_RN_F}^R \\ G_1(\omega)\psi_{11}^E & G_1(\omega)\psi_{12}^E & \cdot\ \cdot & G_1(\omega)\psi_{1N_F}^E \\ \cdot & \cdot & \cdot\ \cdot & \cdot \\ G_{N_E}(\omega)\psi_{N_E1}^E & G_{N_E}(\omega)\psi_{N_E2}^E & \cdot\ \cdot & G_{N_E}(\omega)\psi_{N_EN_F}^E \end{bmatrix} \tag{11}$$

Any nonzero solution to Eq. (10) implies linear dependence of as many columns of the mobility matrix as there are nonzero solutions. The rows of the $[\alpha_F]$ matrix are the orthonormal mode elements of the structure at the forcing coordinates, modified by the frequency function $G_n(\omega)$ for each mode at the frequency of interest. (This frequency function assumes unity values for the rigid-body modes.) Note that the $[\alpha_F]$ matrix is, in general, a rectangular matrix.

If $N_F > (N_R + N_E)$, i.e., if one is attempting to calculate more forces than there are significantly participating structural modes at some frequency, there automatically exist $N_F - (N_R + N_E)$ elements of the $\{\beta\}$ vector that can be arbitrarily chosen to satisfy Eq. (10). This renders that many columns of the mobility matrix linearly dependent, as far as the physical content is concerned. This linear dependence may be disguised by measurement errors, resulting in numerical independence, which naturally leads to erroneous estimates of the vibratory loads. This situation varies with frequency, since at different frequency ranges, different combinations of elastic modes, along with the rigid-body modes (if any), will dominate the structural mobilities. It is also clear from Eq. (11) that the $[\alpha_F]$ matrix is badly behaved at the natural frequencies of lightly damped elastic modes.

When $N_F \leq (N_R + N_E)$, the only possible solution to Eq. (10) is for the vector $\{\beta\}$ to vanish, thus assuring that the columns of the mobility matrix $[Y(\omega)]$ are all linearly independent. The limiting criterion guaranteeing the vanishing of all the elements of the $\{\beta\}$ vector is that there exist at least N_F significant rows in the $[\alpha_F]$ matrix. In order to measure the significance of a row, some norm of that row can be compared to the norm of the most significant now in the matrix. Let a norm of the pth now of the $[\alpha_F]$ matrix be defined as

$$\alpha_{F,p} = \sum_{j=1}^{N_F} (\alpha_{F,pj})(\alpha_{F,pj})^* \tag{12}$$

where $(\alpha_{F,pj})$ is the element at the pth row and jth column of the matrix, and $(\alpha_{F,pj})^*$ is its complex conjugate. These norms can be rearranged according to their size, such that

$$\alpha_{F,1} > \alpha_{F,2} > \ldots > \alpha_{F,N_R+N_E}$$

A measure of the significance of the N_Fth norm, defined as

$$\epsilon_F(\omega) = \ln(\alpha_{F,N_F}/\alpha_{F,1}) \tag{13}$$

can indicate whether or not there are up to N_F significant rows in the $[\alpha_F]$ matrix. $\epsilon_F(\omega)$ is a number that is always negative. Its value for the most significant row is zero. A large negative value indicates an insignificant row. Given that random measurement errors will always permit the numerical pseudoinversion of the mobility matrix $[Y(\omega)]$, an examination of the value of $\epsilon_F(\omega)$ should indicate the reliability of the excitation forces determined by such pseudoinversion for a given number of forces at some desired frequency.

As far as the rows of the mobility matrix are concerned, it is clear that the number of response coordinates must be at least as many as the number of forces. For least-squares estimates, the response coordinates should considerably outnumber the forces. The selection of the response coordinates must be such that at least N_F rows of the mobility matrix are linearly independent in the physical sense. If there are less than N_F independent rows in the mobility matrix, estimates of the dynamic forces will be in error, no matter how many rows there are altogether.

Considerations similar to the foregoing paragraphs can be used to establish a parameter $\epsilon_A(\omega)$ similar to $\epsilon_F(\omega)$ but defined with respect to a matrix $[\alpha_A]$, which is just like the matrix $[\alpha_F]$ except that the rows are constituted by the orthonormal mode elements at the response locations. The lesser of $\epsilon_F(\omega)$ and $\epsilon_A(\omega)$ is the one that should be considered critical to the accuracy of the overall force determination process, i.e.,

$$\epsilon(\omega) = \min(\epsilon_F(\omega), \epsilon_A(\omega)) \tag{14}$$

Numerical Results

In order to confirm some of the practical implications of the foregoing theoretical observations, a numerical study was undertaken. The forced response of two uniform beams, one cantilevered and the other free-free, was simulated numerically. The cantilever beam is deprived of all rigid-body contributions to displacement-type response, a property of such structures as flexible buildings, windmill towers, and turbine blades. The free-free beam retains the rigid-body contributions to its displacement response, much like free-flying structures such as helicopters and airplanes. Fourteen evenly spaced points on the beams were taken as response measurement locations, with excitation forces applied at 1, 2, 3, or 4 selected points as shown in Fig. 1.

The orthonormal mode elements at the response coordinates (which also includes the set of excitation coordinates) were computed from known exact solutions of beam flexural modes.[11]

$$\psi_{nj} = \phi_n(x_j/L) \Big/ \left[\int_0^1 \phi_n^2(x/L)\,d(x/L) \right]^{1/2} \tag{15}$$

where x_j/L is the dimensionless distance of the jth response location from one end of the beam and $\phi_n(x/L)$ is the mode shape value at the specified location.

For the cantilevered beam, there are no rigid-body modes. The elastic-mode shapes are given by[11]:

$$\begin{aligned}\phi_n^C(x/L) = &\{\sin(\beta_n L) - \sinh(\beta_n L)\}\{\sin[(\beta_n L)x/L] \\ &- \sinh[(\beta_n L)x/L]\} + \{\cos(\beta_n L) + \cosh(\beta_n L)\} \\ &\times \{\cos[(\beta_n L)x/L] - \cosh[(\beta_n L)x/L]\}\end{aligned} \tag{16}$$

corresponding to natural frequencies $\omega_n = (\beta_n L)^2 \times \sqrt{(EI/ML^4)}$ where EI is the flexural rigidity of the beam, M is the mass per unit length, and $\beta_n L$ are the solutions to

$$\cos(\beta_n L)\cosh(\beta_n L) = -1 \tag{17}$$

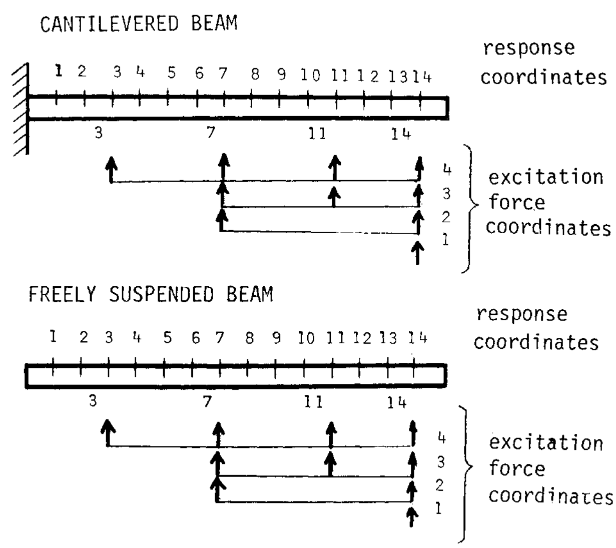

Fig. 1 Response and excitation coordinates for cantilevered and freely suspended beams.

Table 1 Modes of uniform cantilevered beam

			Elastic orthonormal modes					
		Frequency[a]	3.516	22.034	61.701	120.912	199.855	298.564
		Damping	.005	.005	.005	.005	.005	.005
STA	1		−.015	−.080	−.218	−.298	−.764	−.819
STA	2		−.057	−.282	−.690	−.823	−1.766	−1.504
STA	3		−.124	−.549	−1.162	−1.107	−1.650	−.670
STA	4		−.213	−.830	−1.434	−.910	−.306	.876
STA	5		−.322	−1.076	−1.388	−.287	1.240	1.356
STA	6		−.447	−1.247	−1.011	.463	1.743	.219
STA	7		−.586	−1.314	−.391	.967	.801	−1.180
STA	8		−.737	−1.259	.313	.971	−.805	−1.180
STA	9		−.897	−1.076	.911	.479	−1.752	.221
STA	10		−1.064	−.771	1.238	−.251	−1.262	1.361
STA	11		−1.236	−.362	1.191	−.832	.248	.894
STA	12		−1.411	.128	.759	−.944	1.501	−.609
STA	13		−1.588	.672	.013	−.484	1.386	−1.307
STA	14		−1.767	1.244	−.922	.407	−.208	−.196

[a]Dimensionless frequency $\bar{\omega}=\omega/\sqrt{((EI)/(ML^4))}$.

Table 2 Modes of freely suspended beam

		Rigid-body orthonormal modes			Elastic orthonormal modes					
				Frequency[a]	22.373	61.670	120.912	199.855	298.564	416.976
				Damping	.005	.005	.005	.005	.005	.005
STA	1	1.000	−1.501		1.172	.738	.367	.159	−.152	−.472
STA	2	1.000	−1.270		.655	−.013	−.437	−1.046	−1.046	−1.152
STA	3	1.000	−1.039		.166	−.612	−.852	−1.133	−.486	.219
STA	4	1.000	−.808		−.271	−.961	−.750	−.187	.717	1.301
STA	5	1.000	−.577		−.629	−1.001	−.225	.952	1.091	.337
STA	6	1.000	−.346		−.883	−.745	.435	1.321	.177	−1.157
STA	7	1.000	−.115		−1.015	−.274	.881	.607	−.945	−.817
STA	8	1.000	.115		−1.015	.274	.881	−.606	−.945	.817
STA	9	1.000	.346		−.883	.744	.434	−1.321	.177	1.156
STA	10	1.000	.577		−.629	1.001	−.225	−.952	1.090	−.334
STA	11	1.000	.808		−.271	.961	−.751	.187	.716	−1.273
STA	12	1.000	1.039		.166	.612	−.852	1.133	−.491	−.167
STA	13	1.000	1.270		.655	.013	−.436	1.045	−1.034	.835
STA	14	1.000	1.501		1.172	−.738	.368	−.154	−.157	.000

[a]Dimensionless frequency $\bar{\omega}=\omega/\sqrt{((EI)/(ML^4))}$.

Table 1 gives numerical values for the first six orthonormal mode elements of a uniform cantilevered beam at the 14 response locations specified in Fig. 1. A uniform modal damping of $g_n=.005$ [see Eq. (4)] has been assumed.

In addition to elastic modes, the free-free beam, moving laterally in two dimensions has two rigid-body orthonormal modes.

$$\psi_{1j}^R=1, \quad \psi_{2j}^R=[(x_j/L)-\tfrac{1}{2}](\sqrt{12}) \qquad (18)$$

The elastic mode shapes are

$$\phi_n^F(x/L)=\{\cos(\beta_nL)-\cosh(\beta_nL)\}\{\sin[(\beta_nL)x/L] + \sinh[(\beta_nL)x/L]\}-\{\sin(\beta_nL)-\sinh(\beta_nL)\} \times\{\cos[(\beta_nL)x/L]+\cosh[(\beta_nL)x/L]\} \qquad (19)$$

at natural frequencies $\omega_n=(\beta_nL)^2\sqrt{(EI/ML^4)}$

Here, the β_nL are solutions to

$$\cos(\beta_nL)\cosh(\beta_nL)=1 \qquad (20)$$

Numerical values for the rigid-body orthonormal modes of the free-free beam and those for its first six elastic modes are given in Table 2. Uniform modal damping of .005 has also been assumed.

For the four anticipated excitation coordinates, data from Tables 1 and 2 were used to generate the (14×4) matrix of acceleration mobilities $[Y(\omega)]$ for both beams using Eqs. (3-6). These mobilities were considered the true, error-free mobilities of the structures. They were the ones used to generate response accelerations $\{y\}$ using Eq. (1). Of course, the columns of the mobility matrix used for each calculation correspond to the locations and number of excitation forces. It was then supposed that the acceleration mobilities available for force determination were those measured from vibration testing, which were presumed to differ from the true mobilities by some random fraction of the largest mobility in each column.

$$Y_{ij}^{\prime}(\omega)=Y_{ij}(\omega)+E_{ij} \qquad (21)$$

For example, if the size of the largest element in the jth column of $[Y(\omega)]$ was $|Y|_j$ and if ρ_i was a number $(-1\le\rho_i\le1)$ randomly generated by mixed multiplicative congruential method,[12,13] then,

$$E_{ij}=(\rho_i\,|Y|_j)(\gamma/100) \qquad (22)$$

where γ was the percentage error level. The elements $[Y_{ij}(\omega)]$ were assembled into the $(14\times N_F)$ matrix $[Y'(\omega)]$, which was then used in conjunction with Eq. (2) to calculate the applied forces $\{F'\}$. N_F, the number of applied forces,

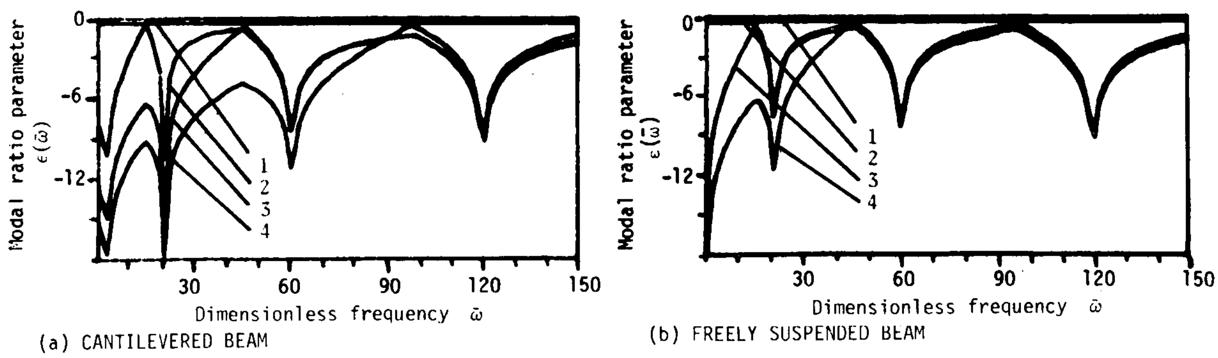

Fig. 2 Modal ratio parameter (index = number of forces).

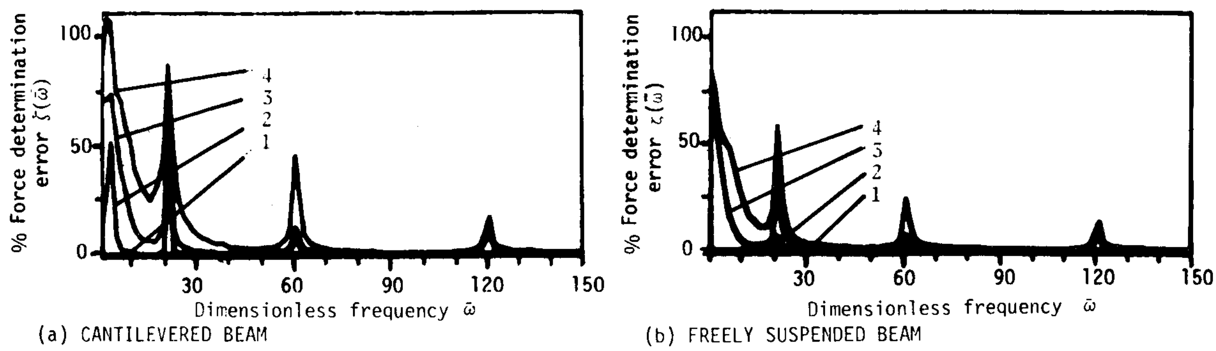

Fig. 3 Force determination error, %; 1% random error in acceleration mobilities (index = number of forces).

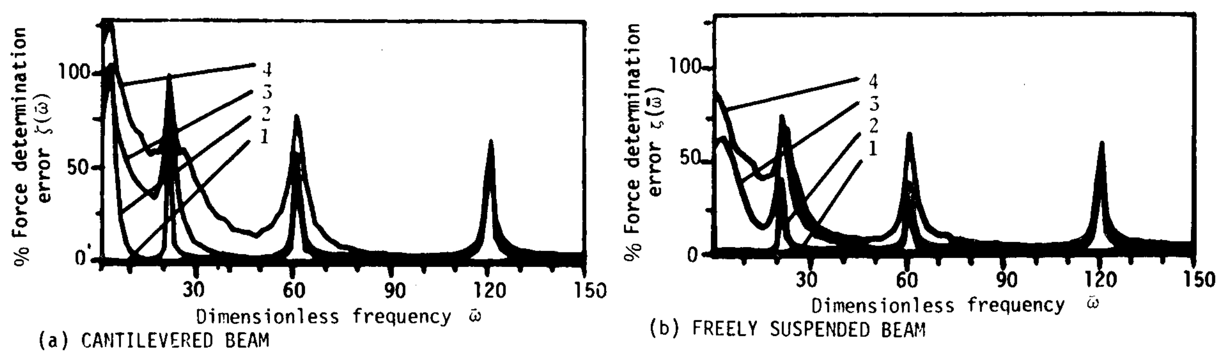

Fig. 4 Force determination error, %; 5% random error in acceleration mobilities (index = number of forces).

was varied from 1 to 4 according to the schematic of Fig. 1. For each value of N_F, several force determinations ($S = 100$) were made with different randomly determined magnitudes and phases for each of the forces. The average error of force determination was calculated at each frequency as

$$\zeta(\omega) = \frac{1}{SN_F} \sum_{s=1}^{S} \left(\sum_{n=1}^{N_F} \frac{|F_n - F_n'|}{|F_n|} \right)_s \tag{23}$$

where | | is the magnitude of the enclosed complex quantity and F_n is the nth element of the force vector.

The results of calculations for dimensionless frequency $1 \le \bar{\omega} \le 150$ are shown in Figs. 2-5. Figures 2a and 2b are plots of modal ratio parameter defined in Eq. (14) for the cantilevered beam (Fig. 2a) and the free-free beam (Fig. 2b), corresponding to $N_F = 1$, 2, 3, and 4. Figures 3-5 are plots of the average error of force determination defined in Eq. (23) for 1, 5, and 15% error levels in the acceleration mobilities, respectively. Figures 3a, 4a, and 5a are for the cantilevered beam, while 3b, 4b, and 5b are for the free-free beam. The four curves in each plot correspond to $N_F = 1$, 2, 3, and 4.

Discussion of Results

The trend of the modal ratio parameter $\epsilon(\omega)$ plotted in Figs. 2a and 2b, as frequency is varied, foretells the frequency domains where the accuracy of force determination will or will not be acceptable. When $\epsilon(\omega)$ falls below a certain level, depending upon the number of forces being calculated, the error of force determination $\zeta(\omega)$ increases. For a given threshold on $\epsilon(\omega)$, it is observed from Figs. 2a and 2b that at certain frequency domains one can accurately determine only a limited number of forces. The number of forces that can be determined with acceptable accuracy are those for which $\epsilon(\omega)$ lies above the threshold value. Note that the curves of Figs. 2a and 2b can be generated ahead of any force-determination process. These curves are dependent only on the orthonormal mode properties of the structure.

Suppose that the error of acceptable force determination is set at a value not to exceed the error present in the measurement of mobilities. In Fig. 3, this value is 1%, in Fig. 4 it is 5%, and in Fig. 5 it is 15%. It is found that the same threshold of approximately $\epsilon(\omega) > -3$ can be established for knowing ahead of time for which frequency domains this

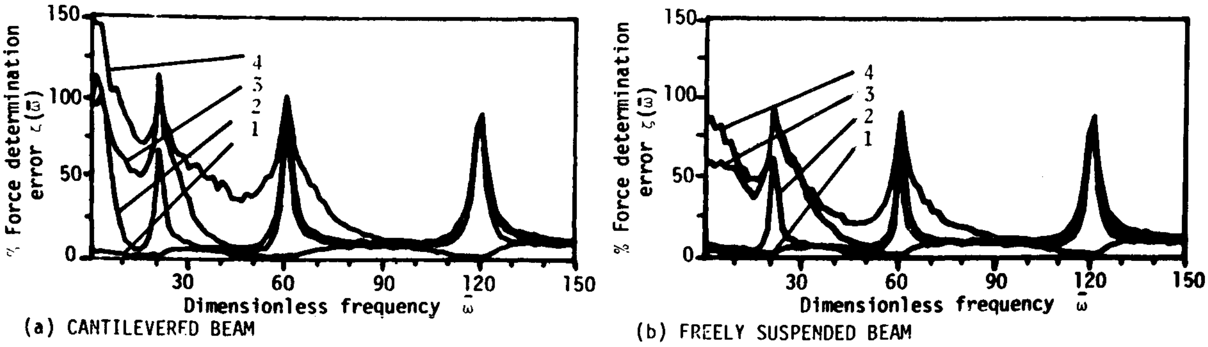

Fig. 5 Force determination error, %; 15% random error in acceleration mobilities (index = number of forces).

Table 3 Domains of feasibility of force determination for uniform cantilevered and freely suspended beams, for dimensionless frequency[a] $0<\bar{\omega}<150$

Number of forces, N_F	Cantilevered beam[b]	Freely suspended beam[b]
	Dimensionless frequency bands	
1	All frequencies	All frequencies
2	(6-20), (24-56), (70-114), (130-150)	(0-20), (25-58), (67-115), (130-150)
3	(33-56), (70-114), (130-150)	(9-20), (25-58), (67-115), (130-150)
4	(78-116), (130-150)	(32-58), (67-115), (130-150)

[a]Dimensionless frequency $\bar{\omega}=\omega\sqrt{((EI)/(ML^4))}$. [b]Uniform modal damping of $g_n = .005$ for all elastic modes assumed.

will be possible, for a given number of forces. For this case, an approximate table of these frequency ranges is presented in Table 3, based on the results of Figs. 2-5.

The biggest difference between the results for the cantilevered and free-free beams can be observed at lower values of the dimensionless frequency ($\bar{\omega}<90$). The existence of the two additional rigid-body modes of the free-free beam already permits the determination of at least two forces at very low frequencies, which is impossible for the cantilevered beam. The lowest frequency at which a given number of forces can be determined is always significantly less for the free-free beam than for the cantilevered beam.

The sharp drops in the $\epsilon(\omega)$ values around the resonances of the elastic modes of both beams is not unexpected. These are regions in which the response of the resonant mode dominates all the other modes. In these regions, no more than one excitation force can be determined with acceptable accuracy. The width of the frequency domains affected by resonant mode effects is obviously dependent on the damping level of the mode.

Conclusions

Some fundamental considerations of modal analysis and linear algebra have been used to establish certain theoretical criteria for assessing the expected accuracy of the method of force determination described herein. These theoretical results were confirmed by numerical calculations based on two uniform beams, one cantilevered and the other free-free.

The presence of finite random errors in the measured acceleration mobilities can set a lower limit on the significance of the modes that must participate in the measured response in order that the determination of a given number of forces be feasible. The theoretical results permit a predetermination of the frequency domains within which the determination of a desired number of forces can be feasible to some level of accuracy.

Comparisons of the results of the cantilever and free-free beams show that freely suspended objects permit more forces to be determined at the lower frequencies than constrained objects. This is a consequence of the presence of rigid-body modes in the response of the free object. In any case, a thorough survey and determination of the orthonormal modes and modal properties of a structure is highly recommended prior to the implementation of such a force-determination scheme.

Acknowledgment

Computational facilities for this research were provided by the University of Maryland Computer Center.

References

[1]Allemang, R. J., "Experimental Modal Analysis Bibliography," *Proceedings of the 1st International Modal Analysis Conference*, Orlando, FL, 1982, pp. 714-726.

[2]Goyder, H. G. D., "Methods and Application of Structural Modeling from Measured Structural Frequency Response Data," *Journal of Sound and Vibration*, Vol. 68, No. 2, 1980, pp. 209-230.

[3]Nagy, E. J., "Improved Methods in Ground Vibration Testing," *Journal of the American Helicopter Society*, Vol. 12, April 1983, pp. 24-29.

[4]Ellis, N., "A Technique for Evaluating the Fluctuating Aerodynamic Forces on a Flexible Building," *Proceedings of the International Symposium on Vibrating Problems in Industry*, Keswick, England, April 1973.

[5]Flannelly, W. G., Bartlett, F. D. Jr., and Fossberg, T. W., "Laboratory Verification of Force Determination, A Potential Tool for Reliability Testing," USAAMRDL-TR-76-38, 1977.

[6]Bartlett, F. D. Jr. and Flannelly, W. G., "Model Verification of Force Determination for Measuring Vibratory Loads," *Journal of the American Helicopter Society*, Vol. 24, April 1979, pp. 10-18.

[7]Jones, R., Flannelly, W. G., Nagy, E. J., and Fabunmi, J. A., "Experimental Verification of Force Determination and Ground Flying on a Full Scale Helicopter," USAAVRADCOM-TR-81-D-11, 1981.

[8]Giansante, N., Jones, R., and Calapodas, N. J., "Determination of In-Flight Helicopter Loads," *Journal of the American Helicopter Society*, Vol. 27, July 1982, pp. 58-64.

[9]Ewins, D. J. and Hillary, B., "A Method for Force Determination from Vibration Response Measurements," Imperial College of Science and Technology, London, Lab. Rept., 1980.

[10]Fabunmi, J. A., "Modal Constraints on Helicopter Vibratory Force Determination by the Pseudo-Inverse Technique," *Proceedings of the International Conference on Rotorcraft Basic Research*, Research Triangle Park, NC, Feb. 1985.

[11]Timoshenko, S., Young, D. H., and Weaver, W. Jr., *Vibration Problems in Engineering*, John Wiley & Sons, New York, 1974, pp. 424-426.

[12]Demidovich, B. P. and Mason, I. A., *Computational Mathematics*, Mir Publishers, Moscow, 1973, p. 653.

[13]Carnahan, B., Luther, H. A., and Wilkes, J. O., *Applied Numerical Methods*, John Wiley & Sons, New York, 1969, p. 588.